MEMORIA DEL TRABAJO DE FIN DE GRADO

GRADO EN FÍSICA

FORMACIÓN DE GALAXIAS CON SIMULACIONES

Juan Carlos Castaño González

Supervised by:

Arianna Di Cintio

Academic course 2023-2024

09-07-2024

Index

Resumen

El modelo Λ-CDM surge del descubrimiento de la aceleración del universo. Este modelo propone una evolución del universo jerárquica, donde primero se generan pequeños cúmulos de materia oscura, seguidos de la formación de halos más grandes que pueden albergar galaxias. Este modelo actualmente es el más utilizado a la hora de desarrollar simulaciones debido a que ofrece una explicación satisfactoria de los datos observacionales a gran escala. Los resultados mostrados en el TFG se han obtenido trabajando con HESTIA (High-resolution Environmental Simulations of The Immediate Area), es un grupo de simulaciones designadas a estudiar el grupo local de galaxias. En el capítulo 2, se estudian los dos halos principales de esta simulación, que son los de la Vía Láctea y Andromeda, donde ciertos resultados, como sus curvas de rotación o su funciones de luminosidad, se han comparado con los datos observacionales de Huang et al., 2016, Chemin et al., 2009 y McConnachie, 2012. Concluyendo que los valores obtenidos por HESTIA se aproximan mucho a la realidad, validando así los resultados que se consigan con esta simulación. Se han obtenido también los perfiles de estrellas, las distribuciones de materia oscura de MW(Vía Láceta) y de M31 (Andrómeda), sus radios viriales y sus galaxias satélites, con las que se han obtendio las respectivas distribuciones radiales.

Utilizando la simulación 37_11 de HESTIA se han encontrado diez galaxias oscuras en un rango entre 1.68 Mpc y 6.4 Mpc de distancia con respecto a la Vía Láctea. Estas galaxias se caracterizan por tener muy poca masa estelar $\sim 10^4$ M$\odot$ en comparación a su masas de gas $\sim 10^6$ M$\odot$ y sobretodo a su masa de materia oscura $\sim 10^9$ M$\odot$. Incluso una de ellas no tiene masa estelar, siendo la primera 'star-less galaxy' encontrada en una simulación. En el capítulo 3, de metodologia y procedimiento, se explican las condiciones que se han aplicado para poder encontrar las galaxias oscuras en la simulación, además, con el objetivo de conocer la configuración que estas galaxias presentan se ha hecho una representación a gran escala de la distribución de los halos de materia oscura, centrada en la Vía Láctea y se han representado las galaxias oscuras con sus posiciones relativas a MW.

En el capítulo 4 de resultados y discusiones, se muestra información relevante de estas galaxias, sus números de partículas de gas, de materia oscura y de estrellas además de sus respectivas masas. Ninguna de las galaxias tienen más de 10 partículas de estrellas, debido a que fue una de las condiciones impuestas a la hora de hallarlas. Se han representado las distribuciones de materia oscura de cada una de las galaxias junto con sus estrellas (en el caso de tenerlas), con el objetivo de conocer el tamaño de sus halos de materia oscura y la disposición de las estrellas en dichos halos. Además, para aquellas galaxias que son galaxias satélites, se han hecho un zoom-out para poder apreciar el halo de materia oscura de la galaxia 'madre'. También se obtuvieron las coordenadas que las galaxias oscuras tienen en la simulación y se calcularon sus distancias relativas a la Vía Láctea y Andrómeda, obteniendo sus respectivas distribuciones radiales.

Se ha representado la relación de masa estelar y masa del halo de materia oscura de cada una de las galaxias oscuras, comparándolas con la media de las relaciones de masa estelar

y masas de halo que suelen presentar las galaxias en general. Esto se ha realizado con el objetivo de visualizar que tan peculiares son estas galaxias con respecto a la falta de masa estelar, pero se ha concluido, que salvo dos casos que si son más especiales, las demás tienen un comportamiento bastante próximo a la media. Los casos exepcionales corresponden, en primer lugar, a una galaxia que tiene mucha menos masa de halo que la que le correspondería teniendo en cuenta la masa estelar que tiene, en segundo lugar, se trata de la galaxia sin masa estelar, teniendo un comportamiento completamente alejado de la media.

Se han obtenido sus halos de gas y se han calculado histogramas que relacionan el número de partículas de gas con la temperatura que presentan. Con la aparente escasez de estrellas que tienen estas galaxias, se ha buscado una explicación estudiando la temperatura que tiene el gas. La temperatura que poseen las partículas de gas resulta ser fría, luego, el gas podría generar estrellas, sin embargo, antes de sacar conclusiones se debe analizar la densidad de dicho gas. En HESTIA, la densidad a partir de la que el gas puede generar estrellas está determinada, siendo n_{thres}= 0.13 $[\frac{amu}{cm^3}]$. Luego de analizar la densidad de gas de las galaxias oscuras, se ha concluido que estas no superan el límite, por lo tanto, no se puede producir la generación de estrellas. Este resultado concuerda con los datos obtenidos en la relación de masa estelar y masa del halo. Por ende, lo verdaderamente curioso de estas galaxias es el estado en el que se encuentra el gas, que a pesar de ser frío es poco denso. Futuros estudios se podrían centrar en analizar el trayecto de estas galaxias y qué interacciones han tenido para presentar las características que tienen. Además, debido a que presentan cantidades de HI (hidrógeno neutro) en torno a 10^6 M$\odot$, es posible que surveys como ALFALFA puedan detectar galaxias con propiedades parecidas a las estudiadas en este TFG.

1. Introduction

Siempre se ha tenido la duda de cuánta es la masa mínima que puede tener una galaxia, recientes descubrimientos de galaxias con muy poca masa estelar han motivado el presente estudio, en la busqueda de ese tipo de galaxias en el grupo de simulaciones HESTIA.

1.1. Λ-CDM model

The Lambda-CDM model arises from the discovery of the accelerating expansion of the universe. This model proposes that the formation of galaxies follows a specific order, with the small clumps of dark matter being generated first, followed by the formation of larger halos which can host galaxies (White y Rees, 1978), and implements the minimal modifications necessary to account for the observed phenomenology with good accuracy.

- In the field of relativity, a term incorporating the **cosmological constant** was introduced into the field equations.($\Lambda \sim 10^{-52} m^{-2}$).

$$R_{\mu v} - \frac{1}{2} R_{\mu v} + \Lambda R_{\mu v} = \frac{8\pi G}{c^4} T_{\mu v}$$

  This term accounts for the repulsive character of gravitation on large spatial scales, where the energy density of the universe is very low, leading to an acceleration of the universe.

- In order to account for the observational dynamics of the universe, a new component is added to the source of the gravitational field, **dark matter**, which only interacts gravitationally, does not absorb, reflect or emit electromagnetic energy.

This model offers a satisfactory explanation of the large-scale observational data. However, discrepancies emerge when the study is carried out at small galactic scales ($M_{star} < 10^9 M\odot$). This is because the predictions obtained by numerical simulations based on the Lambda-CDM model do not align with the real observations. This discrepancy is commonly referred to as the *small-scale cosmology crisis*. The cases in which it occurs are as follows:

- *Missing satellite problem* (Klypin et al., 1999), N-body simulations show that the approximate number of subhalos, which can host dwarfs satellite galaxies, orbiting both the Milky Way and other galaxies such as Andromeda is around a thousand (Moore et al., 1999). However, this does not agree with the observational results, where the number of dwarfs galaxies orbiting both MW and M31 is much lower. Among the explanations given, one option could be that the interaction between dark matter and baryonic matter modifies the structure of the subhalo, thus reducing the number of observable dwarfs galaxies due to e.g. tidal stripping.

- *Cusp − core problem* consists of the discrepancy between the dark matter density profiles predicted by the Lambda-CDM model with respect to cosmological observations of matter distribution in small-scale galaxies. For the Lambda-CDM case, the dark matter density profiles indicate that the distribution of dark matter halos is cusp-shaped, indicating that at the centre of the halo there is a sharp increase in dark matter density. However, observations that have been made of galaxy rotation curves indicate that the dark matter halo density profiles are core-shaped (De Blok y Bosma, 2002), meaning that the density remains relatively constant as you move towards the centre of the halo.

- *Planes of satellite problems* . Simulations based on the Lambda-CDM model predict a spherical distribution of dark matter halos that can host satellite galaxies around their host galaxy. However, observational results indicate that in the case of the Milky Way or Andromeda, several of the satellite galaxieshave a planar distribution around these host galaxies, specifically, in the case of MW, the plane in which some (but not all) of the satellite galaxies are located is approximately perpendicular to the disc of the galaxy itself. The problem is that according to the Lambda-CDM model, this type of distribution is very rare, but observationally it has been found to be more common than the model indicates.

This thesis will not explore the limits at which the results of the simulations cease to be similar to those obtained observationally, but it will make use of a specific simulation, HESTIA, therefore, the question of how these simulations work is of interest because it will provide a deeper understanding when explaining the simulation with which the development of this study was carried out.

1.2. Cosmological simulations

Cosmological simulations are computational tools which, through a model (in our case, the Λ-CDM) and initial conditions (distribution of matter and energy immediately after the Big Bang), represent the formation and evolution of galaxies and the universe. These can be classified into two types, hydrodynamical and N-body simulations:

- Hydrodynamic simulations: These simulations use the equations of hydrodynamics, describing the motion and interactions of gas and dust in space. Accurate models are achieved, where, in addition to hydrodynamics, radiation and gravity are taken into account, even complex physical processes such as the formation of black holes are obtained. As a result of such precision, these simulations are both computationally and analytically complex, limiting the spatial resolutions that can be achieved.
- N-body simulations: In these simulations, galaxies are treated as particles and each particle represents a large amount of stellar mass or dark matter. They require less computational power, since the physics being modelled is limited to gravity and the interaction between particles, so large-scale simulations can be obtained more quickly, modelling galaxy formations in large volumes of the universe. Unlike hydrodynamical simulations, these are less detailed in their cosmological evolutions.

The importance of simulations data lies in the conclusions that can be drawn from them. In addition to examining the formation of galaxies, they permit the study of their interactions with the cosmic environment and the factors influencing their shape, size, and composition. They are also usefull for comparing real observations of galaxies with simulated ones, enabling the refinement of models to make them more similar to reality and, consequently, to enhance the accuracy and reliability of future simulations.

1.3. Starless galaxies

As mentioned above, this project was carried out using the Hestia simulation (Libeskind et al., 2020), which has been used to study the existence of galaxies with no stars but with both dark matter and gas, since one question that scientists have been asking for years is: *what is the minimum mass that a galaxy can have?* This analysis is motivated by two recently published papers, where the observational data obtained provide a new perspective on this issue.

The first, Benitez-Llambay y Navarro, 2023 discovered at a distance of about 4.7 Mpc from M94, a system they named Cloud-9 that has properties similar to REonization-Limited H I Clouds (RELHICs), that is, it is a dark matter halo without stars but with gas in hydrostatic and thermal equilibrium with the cosmic ultraviolet background. The dark matter halo in which Cloud-9 is located seems to follow the Navarro-Frenk-White profile (Navarro, 1996), which describes the dark matter density along the halo as a function of radius by this equation:

$$\rho(r) = \frac{\rho_0}{\frac{r}{Rs} + (1 + \frac{r}{Rs})^2}$$

Where Rs is a parameter that varies from halo to halo. Despite a small systematic difference between Cloud-9 and Λ-CDM RELHICs, the correlation between the observed data and the model is sufficiently strong to suggest that Cloud-9 could be the first ever observed RELHIC.

The second, Smith et al., 2024 identifies the least luminous Milky Way satellite galaxy to date, which they have named Ursa Major/UNIONS 1. This galaxy was discovered approximately 10 kpc from the Sun by the Ultraviolet Near Infrared Optical Northern Survey. The absolute magnitude of the V-band (visible band), which is $+2{,}2^{0{,}4}_{0{,}3}$ mag, was used to determine the stellar mass of the galaxy, which was found to be 16^{+6}_{-5} $M\odot$. This mass is considerably smaller than the mass typically associated with galaxies of a similar size, which is approximately 10^5 $M\odot$.

With regard to the galaxies observed in HESTIA, nine of them have been identified, with stellar masses of approximately 10^5 $M\odot$. These are negligible in comparison with the amounts of dark matter present. I proceed to put the last numbers corresponding to the ID of each of the galaxies, because they are the relevant ones, since the first ones are the same for all of them $\#ID = 12700000$: **273,278,370,393,691,746,804,1064** y **5129** . One notable exception is galaxy 398, which lacks any star particles and therefore has a stellar mass of zero: **398** . To identify these galaxies, , a number of filters were applied, including the resolution criterion. This was implemented in order to ensure that all galaxies were of a sufficiently high degree of resolution, as this would facilitate the extraction of more information. The resolution criterion is defined as follows: The fMhires value must exceed 0.98. Furthermore, three of the galaxies in question are satellites of larger galaxies. The different radial distances of these ten galaxies to both the Milky Way and Andromeda have also been found. And images of their dark matter halos have been obtained with the position of the star particles being plotted on top. Concerning the information obtained about MW and M31, their virial radii have been represented, with their respective dark matter halos and their satellite galaxies, as well as a

large-scale image where both these two galaxies and the 10 starless galaxies are represented, differentiating those that are satellites from those that are not.

2. HESTIA Cosmological Simulation

La simulación con la que se ha llevado a cabo el TFG es HESTIA, cuyos halos principales son el de la Vía Láctea (MW) y Andrómeda (M31), en este capítulo se obtienen información sobre estos halos, como sus curvas de rotación, sus perfiles de estrellas, sus galaxias satélites, sus distribuciones de materia oscura, sus radios viriales, sus funciones de luminosidad y sus distribuciones radiales.

2.1. HESTIA

HESTIA (High-resolution Environmental Simulations of The Immediate Area) is a set of cosmological simulations which studies the local group of galaxies. It uses the AREPO code (Springel, 2010; Pakmor et al., 2016), which is used to solve the magnetohydrodynamics equations for a given Voronoi grid. Furthermore, it employs the AURIGA galaxy formation model. (Grand et al., 2017). And the simulations use the best fit Planck Collaboration et al., 2014 values: $\sigma_s = 0.83$, $H_0 = 100\ [\frac{h \cdot km}{s}]$, h = 0.677 , $\Omega_\Lambda = 0.682$; $\Omega_M = 0.318$ for DM only while $\Omega_M = 0.270$ and $\Omega_b = 0.048$ for hydrodynamic.

Among the groups of simulations found in HESTIA, there are intermediate resolution and high resolution, of the latter group there are only three, which are **09_18, 17_11** and **37_11**. The first number refers to the long-wave seed and the second number refers to the short-wave seed. The mass and spatial resolutions that 37_11 have, are the following, $m_{dm} = 1{,}5 \cdot 10^5 M\odot$, $m_{gas} = 2{,}2 \cdot 10^4 M\odot$, $m_{star} \approx 2 \cdot 10^4\ M\odot$ and $\epsilon = 220$ pc. The 37_11 simulations have been used for the data and images in this work.

2.2. Milky Way and Andromeda in HESTIA

The initial focus of our attention was on the Milky Way (MW) and Andromeda (M31), where we obtained star renders in the default position determined by the simulation and in face-on and side-on views. Ussing the Hubble's sequence classification (Hubble, 1979), the Milky Way would have the classification of a SBbc galaxy, which is defined as a barred spiral galaxy with a flat rotating disc, moderately wound spiral arms and a central bulge of considerable size. For Andromeda, its classification is SA(s)b, which is a regular spiral galaxy with clearly defined and moderately convoluted spiral arms.

Their rotation curves have been obtained, where, although a Keplerian decay of the orbital velocity with respect to a distance r from the centre would be expected: $V(r) \propto \frac{1}{\sqrt{r}}$, observationally the data indicate that the decrease of the stellar mass and gas distribution

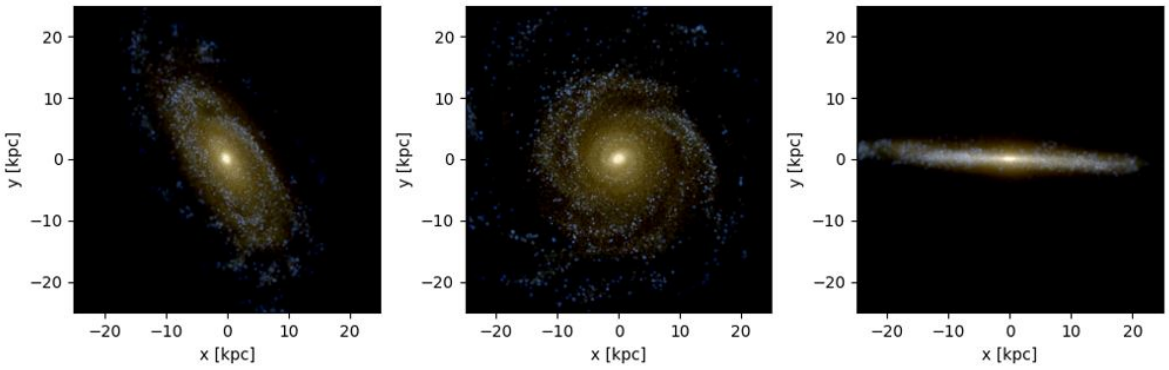

(a) Milky Way

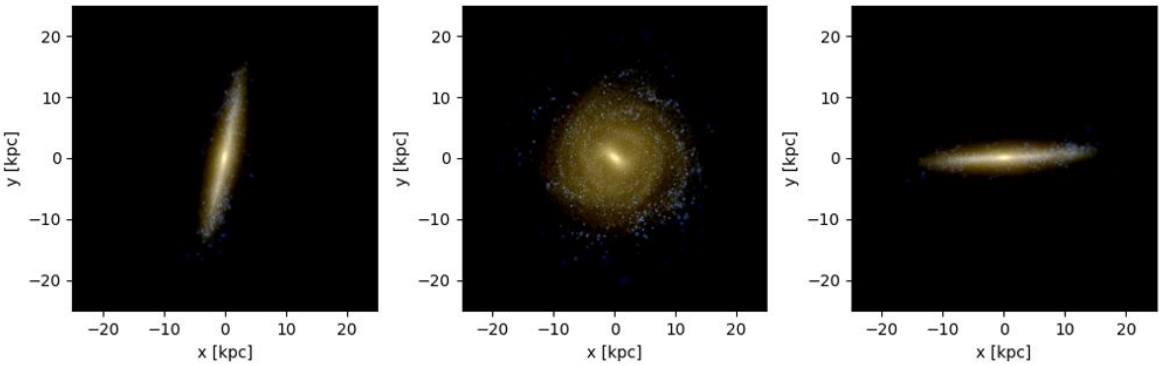

(b) Andromeda

Figure 2.1

remains fairly constant as the distance from the bulge of the galaxy increases, reaching even beyond the visible edge of the galaxy. This behaviour is called a flat rotation curve (Rubin et al., 1978), which is caused by the existence of dark matter, where its presence is markedly higher than that of baryonic matter in the outer region of the galaxy. As can be seen, the observational data obtained by both Huang et al., 2016 and Chemin et al., 2009 are similar to the total MW and M31 rotation curves obtained in HESTIA, where dark matter, stars and gas are taken into account.

With respect to their star profiles, the stellar mass density decreases drastically as one moves away from the bulge of the galaxy, with a slight upturn in the case of M31 at a distance of approximately 60 kpc, while in the case of MW the increase in density is more pronounced and is around 70 kpc away from the centre.

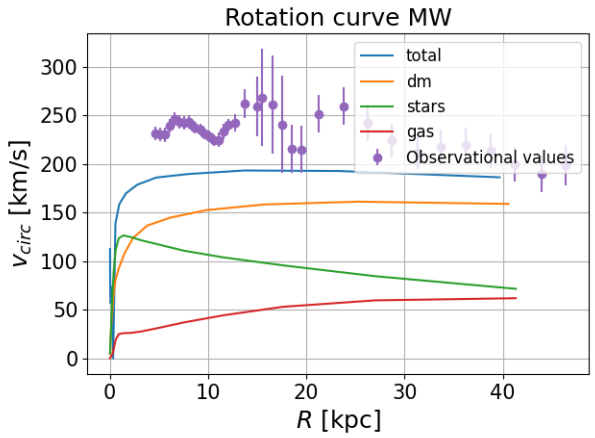

(a) The observational data shown for MW are from Huang et al., 2016

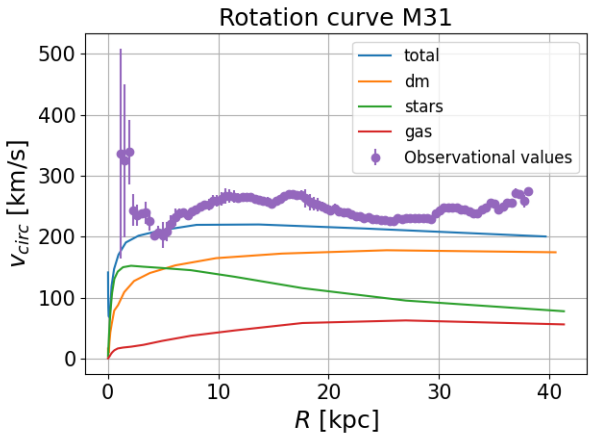

(b) The observational data shown for M31 are from Chemin et al., 2009

Figure 2.2

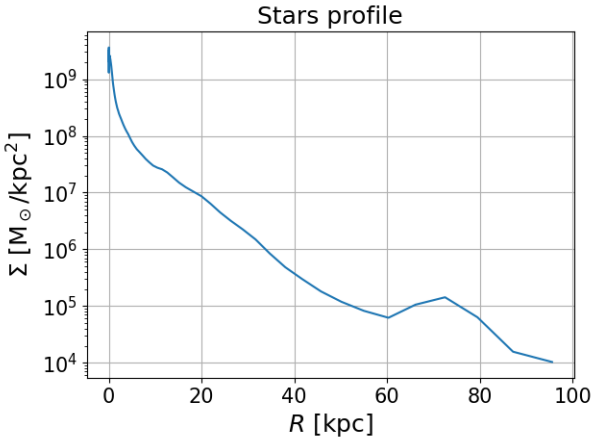

(a) Milky Way

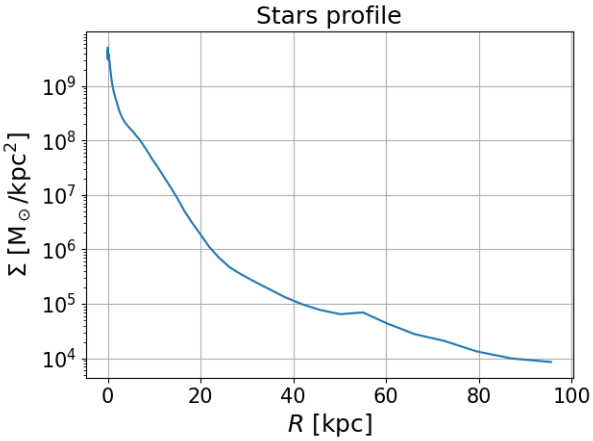

(b) Andromeda

Figure 2.3

2.3. MW and M31 satellite galaxies

A brief study has been carried out into the satellite galaxies, which are smaller galaxies that orbit both MW and M31 and are within their virial radius. This radius is approximately 200 kpc, with the virial radius of Andromeda being slightly smaller than that of the Milky Way. In the case of the Milky Way, sixteen were obtained, with $\#IDs$: **41, 49, 83, 130, 141, 148, 174, 183, 200, 211, 224, 258, 272, 976, 8263, 9146**. In the case of Andromeda, 13 were obtained, with its $\#ID$ being: **91, 99, 104, 147, 342, 396, 501, 502, 1408, 2769, 5278, 7454**. The different conditions that have been applied to obtain these satellite galaxies are:

- Resolution greater than 0.99.
- Number of dark matter particles above 50.
- Number of star matter particles above 50.
- Amount of stellar mass above 10^4 $M\odot$ (previously removing winds).

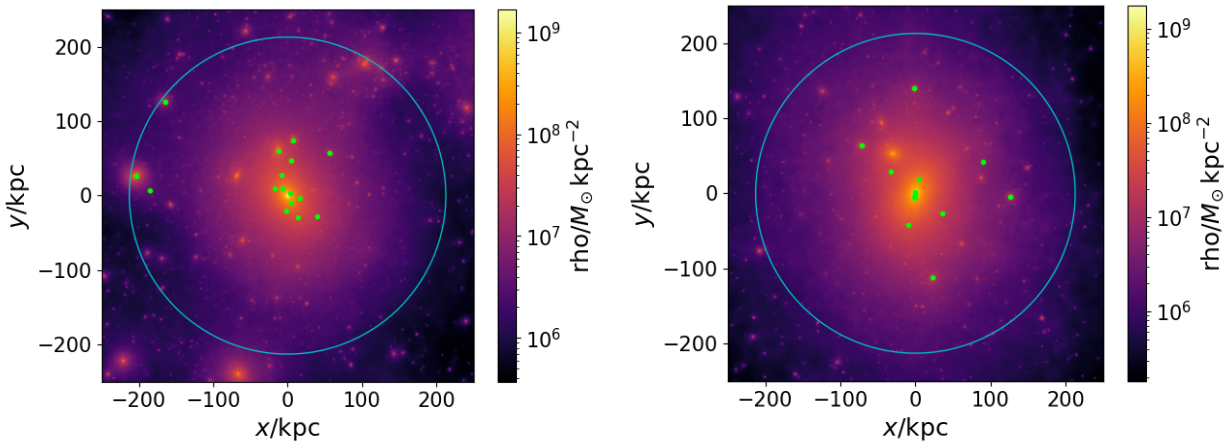

(a) Milky Way

(b) Andromeda

Figure 2.4: Images of the dark matter halos in both galaxies. The bar on the right of each of the images indicates the density of dark matter, the warmer the colours, the higher the density. The virial radius are also shown in blue and the different satellite galaxies in green.

The configuration of satellite galaxies is contingent upon the distribution of dark matter in their "parent"galaxies. It is more probably that these galaxies will be more likely to be found in areas of the halo where there is a higher density of dark matter. This phenomenon also extends to the distribution of stars and gases, which is not random but is determined by the strong gravitational force exerted by dark matter upon them.

The radial distributions of the Milky Way and Andromeda with respect to their satellite galaxies have been obtained, in order to know more accurately the different distances from the centre. In relation to the above, there is a greater presence of galaxies in the central area of the dark matter halo, because the centre of the galaxy is where the highest concentration of dark matter is found. However, this does not imply that there are some of the satellite galaxies that even lie practically at the limit of the virial radius of their parent galaxy, as is the case in MW where there are 3 of these galaxies that are clearly separated from the central group. With respect to M31, the dispersion of galaxies is greater because, although they are not located in the centre as in the case of MW, they are not located at the limits of the virial radius either.

In addition, the luminosity functions of both galaxies have been found. Working with this kind of information, it is possible to analyse the structure and composition of the galaxies,

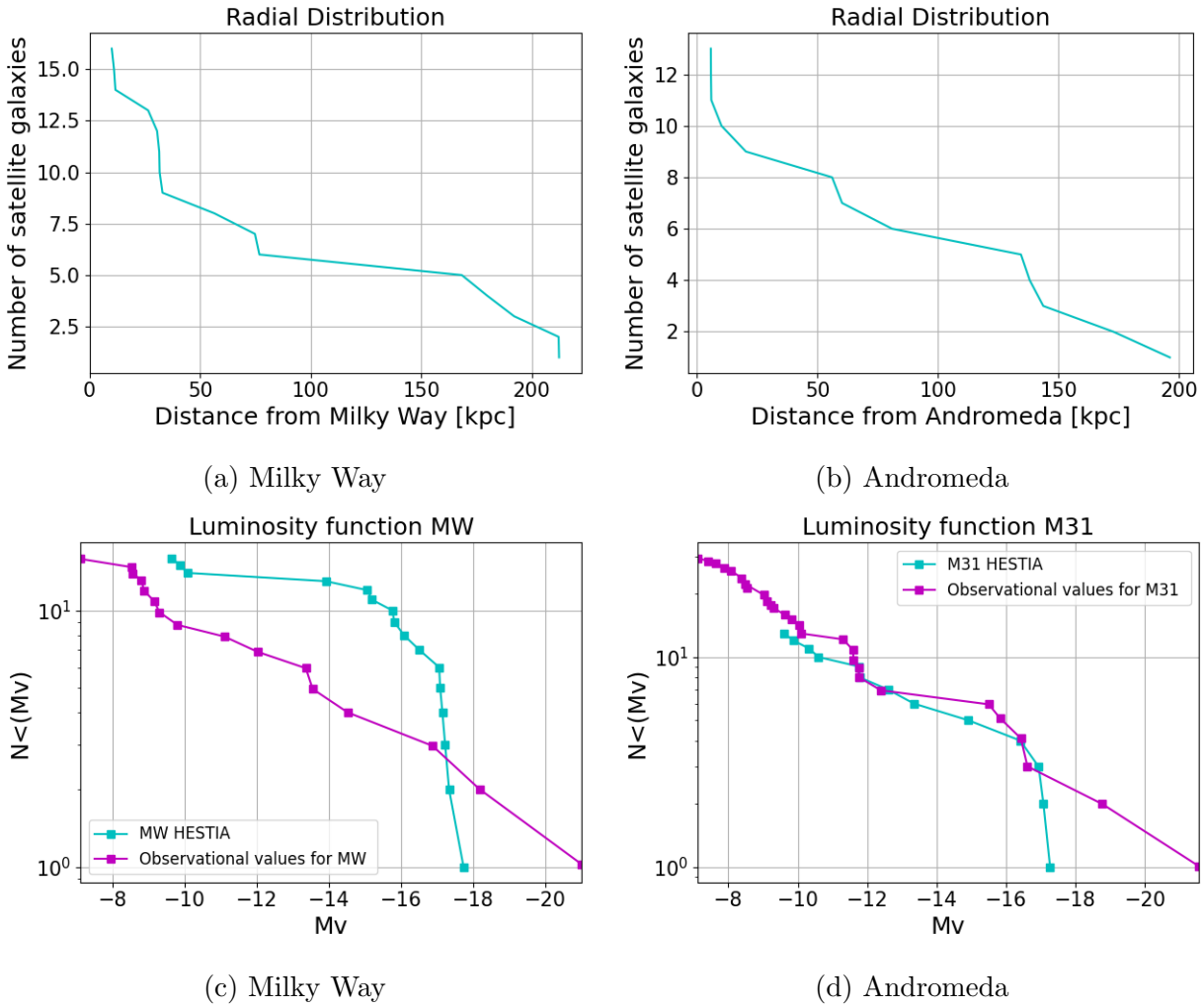

(a) Milky Way

(b) Andromeda

(c) Milky Way

(d) Andromeda

Figure 2.5: The obervational data shown on the luminosity functions of MW and M31 are from McConnachie, 2012

to learn about their evolutionary formation by comparing various luminosity functions at different redshifts, or to know the stellar population and study its evolution. We have also plotted the observational values of the MW and M31 luminosity functions obtained by McConnachie, 2012, in order to compare them with those of 37_11. We conclude that our simulation correctly reproduces the observations.

3. Sample & Metodology

Se han aplicado condiciones para la obtención de las diez galaxias oscuras, como su resolución o el número de partículas de estrellas y de materia oscura. Una de ellas, la más especial, no tiene ni una sola estrella. Además se han hecho dos representaciones, la primera, a gran escala para visualizar la disposición de estas galaxias con respecto a MW y M31, la segunda, para poder apreciar los halos de MW y M31 sin la presencia de halos de baja resolución.

3.1. Selection of dark galaxies

We then proceed to analyse the different galaxies that have very little stellar mass compared to the mass of gas and above all dark matter, known as *dark galaxies*. The conditions that have been imposed are the following:

fMhires > 0.99
DarkMatter Particles > 50
Star Particles $\leqslant 10$
Gas Mass > 0

The galaxies found with these conditions are ten, whose last numbers of the *ID* are : **273, 278, 370, 393, 398, 691, 746, 804, 1064, 5129**. The galaxy with *ID*: **398** is the only one that does not contain any stellar mass, so it is a '*starless*' galaxy. In addition three of them are satellite galaxies of a larger one, these are: **746, 1064, 5129**, whose 'parent' galaxies are, 178, 116, 146 respectively.

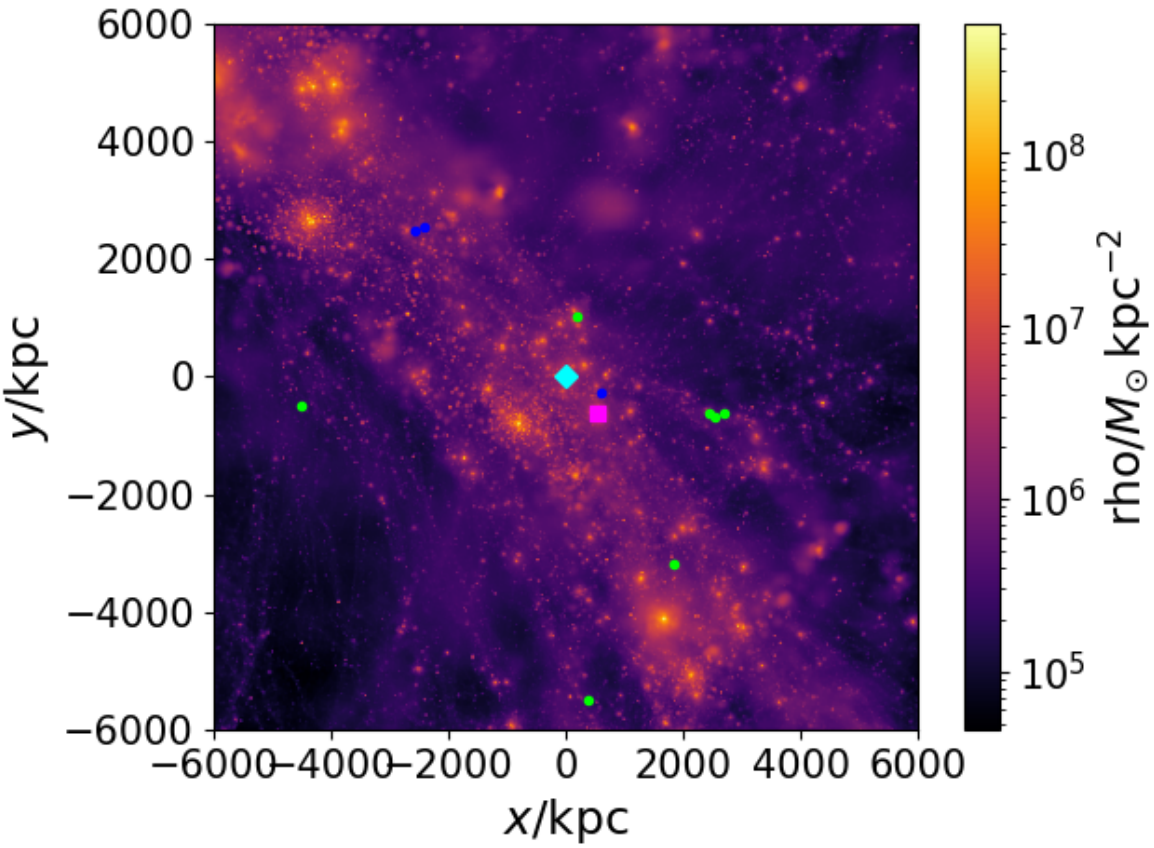

Figure 3.1: DM distribution of the galaxy centred at MW (cyan diamond), showing the galaxy M31 (Magenta square) and the ten dark galaxies, where the blue dots are the galaxies that are satellites of other larger galaxies and the green dots are the other 7 galaxies.

In order to get an overview of the configuration of the dark galaxies with respect to the dark matter distribution, a large-scale picture of the dark matter in the simulation has been obtained. The simulation has been centred on the Milky Way and the positions of both the dark galaxies and Andromeda have been found as a function of the Milky Way. In the image there are high-resolution halos and low-resolution halos, because the scale of the image is very large (12 [Mpc]), large enough for the ten dark galaxies to appear. Low-resolution halos are characterised by larger masses than high-resolution halos. In the image, low-resolution halos can be identified as those with individual particles, an example of which is the one in the first quadrant of the image, just to the left of the two galaxies shown as blue dots. The presence of the low-resolution halos in the image changes the appearance of the high-resolution halos. An example of the alteration in the values of these low-resolution halos would be the halos of MW and M31, which should look much bigger in the final image, but they are hardly noticeable.

The image below has been created to provide a clearer view of what the MW and M31 halos look like without the presence of low-resolution halos. As can be seen, the halos of these two galaxies are the largest with respect to the others in their vicinity. To obtain the image, a specific filter has been applied, whose function is to represent in the image only the halos that are within a sphere of radius 2.5 [Mpc] with respect to MW. This ensures that the low-resolution halos that did appear in the previous image do not appear.

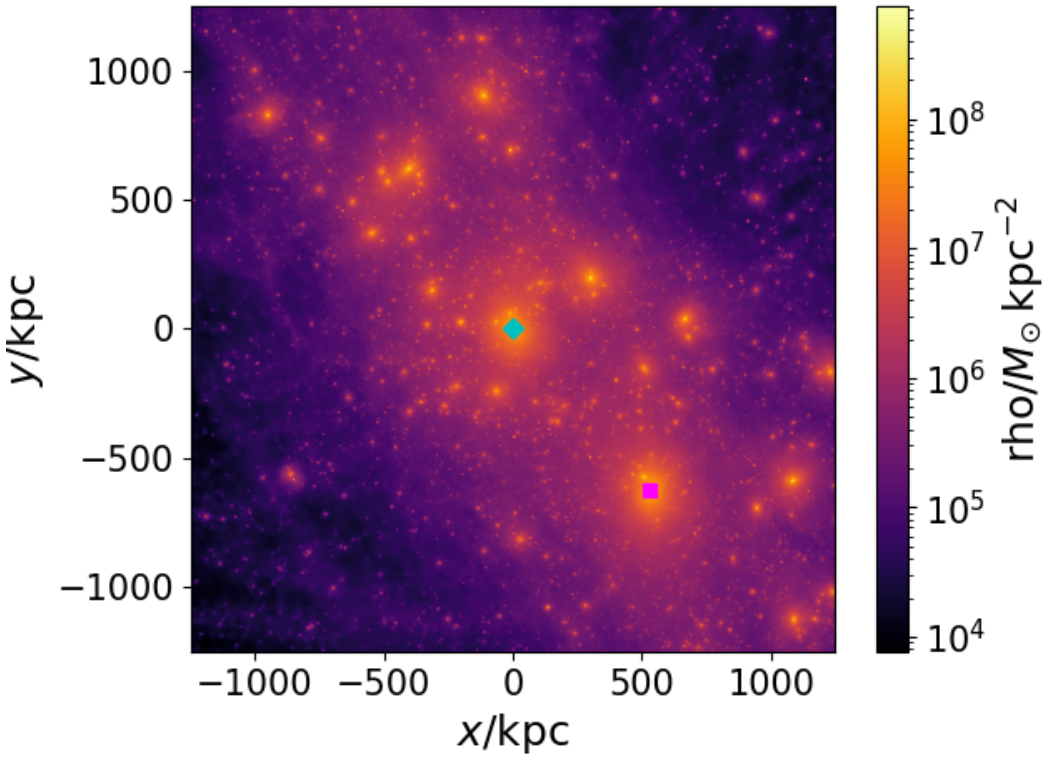

Figure 3.2: DM distribution of the galaxy centred at MW (cyan diamond), showing the galaxy M31 (Magenta square), with a width = 2.5Mpc

4. Results and Discussions

Los resultados obenidos se reparten en tres apartados. El primero consiste en información general de las diez galaxias oscuras, entre la que se encuentra, su número de partículas de estrellas, gas y materia oscura, así como las masas respectivas. Se obtienen tres grupos de imágenes para estas galaxias, la importancia del primer grupo de imágenes recae en el halo de materia oscura de cada una, el segundo grupo de imágenes consiste en hacer un zoom-in a aquellas galaxias que posean estrellas y que en el primer grupo no haya quedado clara la disposición de estas en el halo, por último, el tercer grupo consiste en hacer un zoom-out para poder apreciar aquellas galaxias que son satélites de otras y poder ver claramente el halo de estas en comparación con el halo de su respectiva galaxia 'madre'. El segundo apartado consiste en la obtención de las coordenadas de cada una de estas galaxias y de sus distancias relativas a MW y M31, calculando las distribuciones radiales de las galaxias oscuras a la Vía Láctea y Andromeda, además, se estudia la relación de masa estelar frente a masa del halo de estas galaxias. El tercer y último apartado, consiste en estudiar la temperatura y la densidad que presentan las partículas de gas de las galaxias oscuras, con el objetivo de buscar una explicación a la escaséz de número de estrellas que presentan

4.1. Relevant information of the Dark Galaxies

ĮD	Sub Structure Number	Particle Number	Number Stellar Particle	Star Mass [M⊙ 10^4]	Number DM Particle	DM Mass [M⊙ 10^9]	Number Gas Particle	Gas Mass [M⊙ 10^6]
273	9	25434	1	2.8	25157	5.05	276	9.48
278	7	24726	6	14.94	24719	4.96	1	0.06
370	3	17269	6	17.46	17191	3.45	72	3.19
393	2	16317	3	6.56	15452	3.15	862	29.93
398	3	16051	0	0	15984	3.21	67	2.7
691	0	8744	1	2.59	8742	1.75	1	0.03
746	1	8067	10	22.62	8028	1.61	29	1.1
804	1	7289	4	9.07	7267	1.46	18	0.75
1064	0	5342	2	5.11	5339	1.07	1	0.04
5129	0	1008	2	4.83	937	0.19	69	3.03

Table 4.1: Information on dark galaxies, their substructures, star, dark matter and gas particles, as well as their respective masses in solar masses.

Relevant information has been obtained for each of the dark galaxies to see if they share similarities that may be of interest. As for the number of particles, most of them correspond to dark matter particles, because the presence of dark matter is much higher than that of gas and star particles, which is an expected result due to the nature of the galaxies under study. The same is true for the masses, with the amount of stellar and gas mass in these dark galaxies being several magnitude levels below the amount of dark matter mass. Specifically, the amount of stellar mass that these galaxies contain is around 10^4 $M\odot$, on the other hand, the amount of gas mass that they have oscillates a little more, having between $10^4 M\odot$ and 10^6 $M\odot$. With respect to the dark matter mass, most of them are around 10^9 $M\odot$, except the galaxy with #ID: **5129**, which is the only one with a dark matter mass of 10^8 $M\odot$, this is due to the fact that its number of dark matter particles is clearly lower than the rest. However, although it has far fewer dark matter particles than the others, this number is still higher than the largest number of gas particles, which is 862 particles, and the galaxy that has them is the one with #ID: **393**.

In addition, the dark matter halos of the ten dark galaxies have been obtained, representing also the stars (if any). For some galaxies, such as those in # ID: **278, 370, 393, 746, 804, 1064** and **5129**, they have been represented at different widths, with the aim of being able to appreciate the dark matter halo in its entirety in the first group of images and then to clearly distinguish the configuration of the stars in the second group of images. Moreover, for those dark galaxies that are satellite galaxies (# ID: **746, 1064, 5129**), images have been obtained where the width is wide enough to be able to appreciate their 'mother' galaxies.

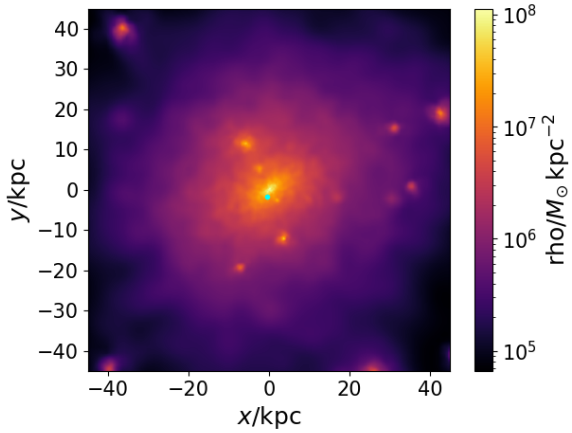

(a) DM distribution of the galaxy with ID: 273; DM in purple and stars in green

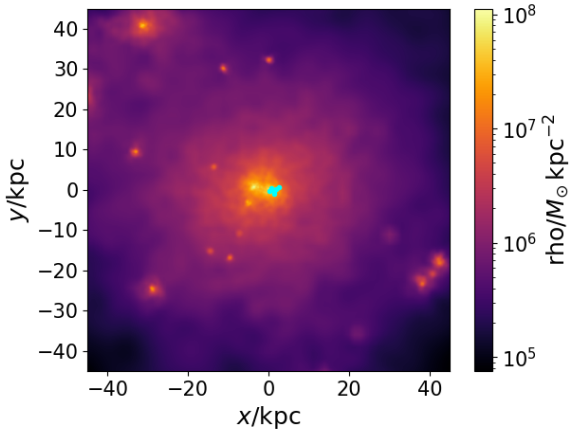

(b) DM distribution of the galaxy with ID: 278; DM in purple and stars in green

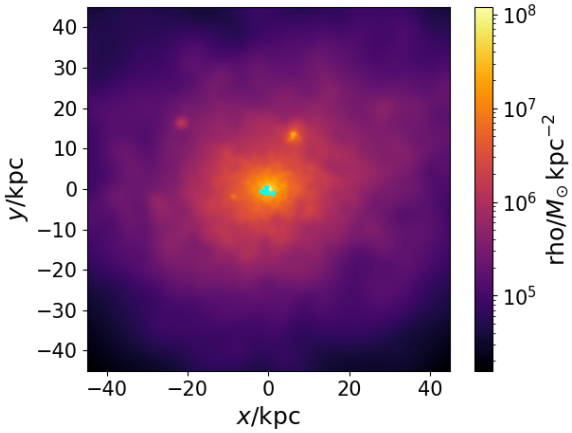

(c) DM distribution of the galaxy with ID: 370; DM in purple and stars in green

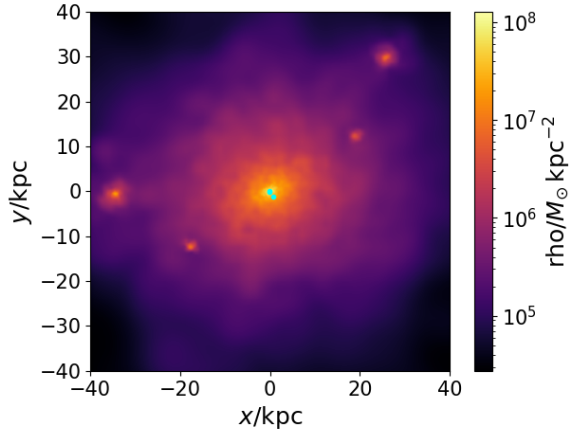

(d) DM distribution of the galaxy with ID: 393; DM in purple and stars in green

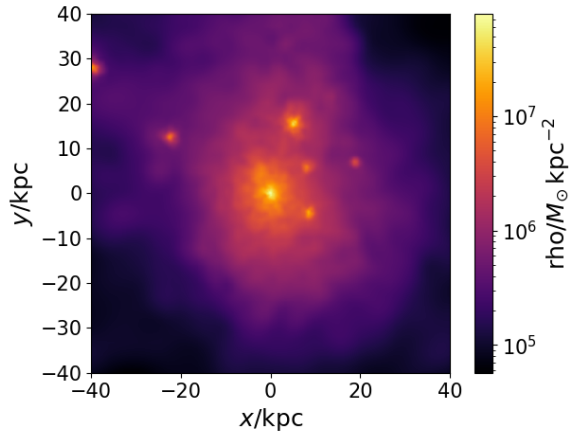

(e) DM distribution of the galaxy with ID: 398; DM in purple and stars in green

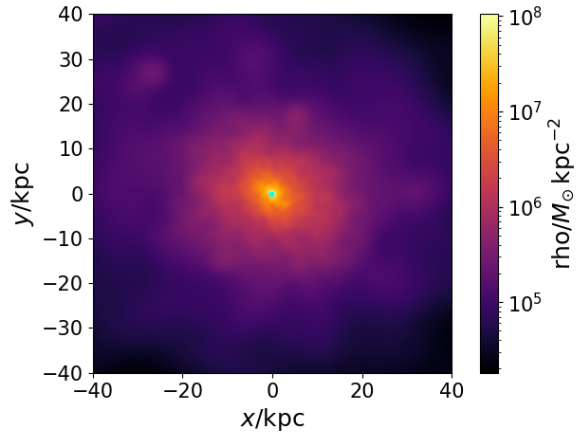

(f) DM distribution of the galaxy with ID: 691; DM in purple and stars in green

Figure 4.1

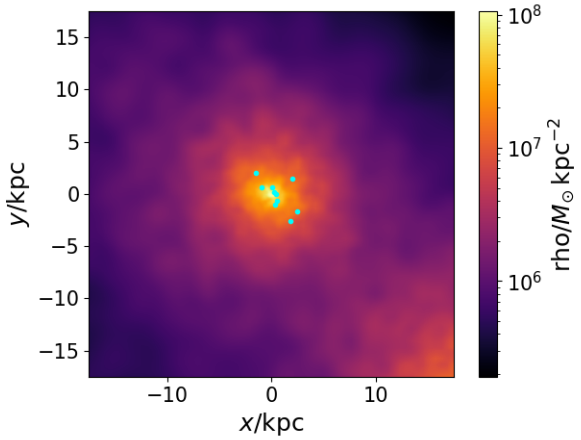

(a) DM distribution of the galaxy with ID: 746; DM in purple and stars in green

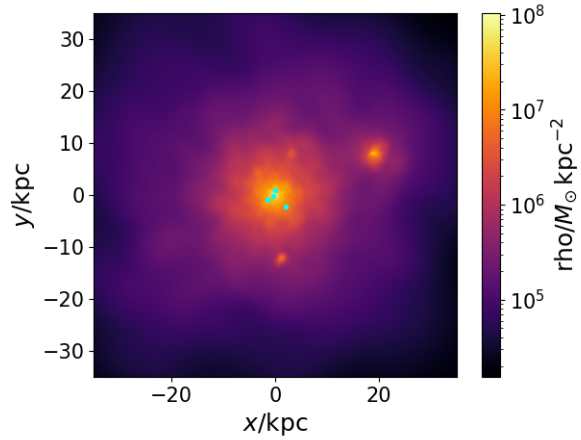

(b) DM distribution of the galaxy with ID: 804; DM in purple and stars in green

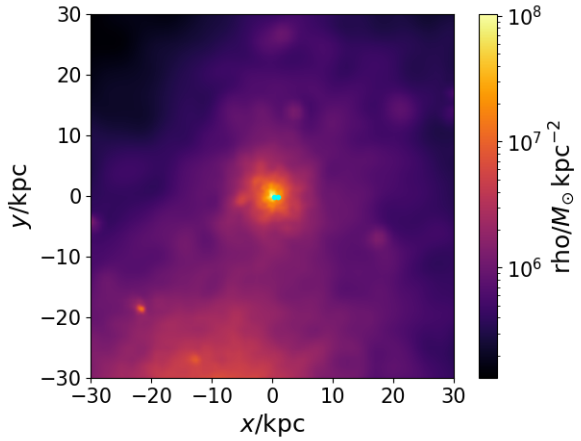

(c) DM distribution of the galaxy with ID: 1064; DM in purple and stars in green

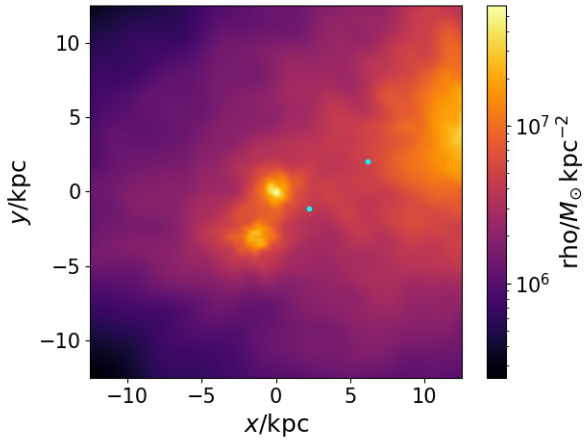

(d) DM distribution of the galaxy with ID: 5129; DM in purple and stars in green

Figure 4.2

The dark matter halos of the galaxies with #ID : **273, 278, 370, 393, 398, 691** are the largest of the group of dark galaxies, with a width of 80 [*kpc*], moreover, except for **691**, the others, apart from having the central zone where the highest concentration of dark matter is found, also have several zones where there is a high density of DM. As for the galaxies with # ID: **746, 804, 1064, 5129**, they have smaller dark matter halos, between 25 [*kpc*] and 50 [*kpc*]. In the case of the satellite galaxies, the halo of the 'mother' galaxy of each of them can be seen, and even in the galaxy **5129** we can see how one of its stars is far from the centre of the halo due to the gravitational influence of the larger halo of the 'mother' galaxy.

Below are the galaxies that have been zoomed-in to show more clearly the configuration of the number of stars they have, indicating the specific width for each case. As expected, the stars are in the centre or near the centre of the dark matter halo, because this is where there is a higher density of DM.

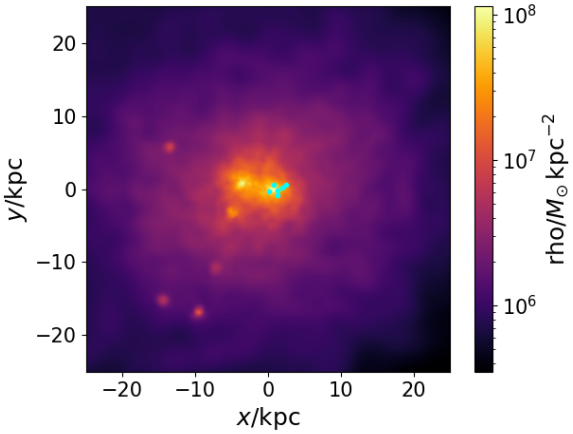

(a) Star configuration of the galaxy ID : 278 with a width = 50 kpc; DM in purple and stars in green

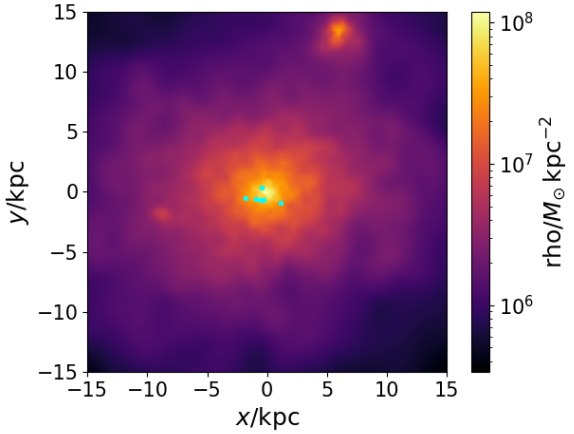

(b) Star configuration of the galaxy ID : 370 with a width = 30 kpc; DM in purple and stars in green

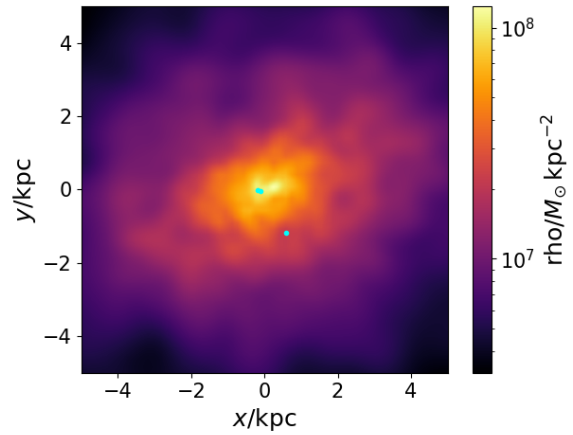

(c) Star configuration of the galaxy ID : 393 with a width = 10 kpc; DM in purple and stars in green

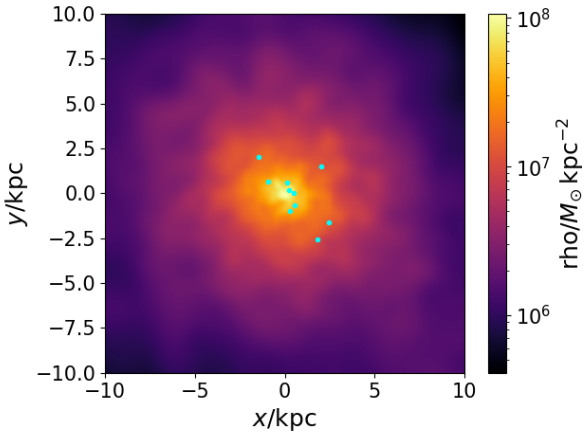

(d) Star configuration of the galaxy ID : 746 with a width = 20 kpc; DM in purple and stars in green

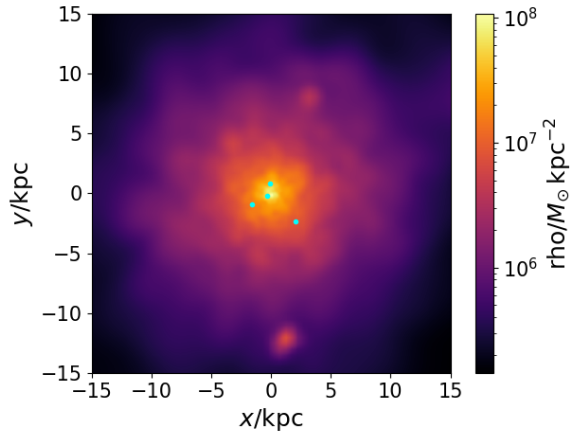

(e) Star configuration of the galaxy ID : 804 with a width = 30 kpc; DM in purple and stars in green

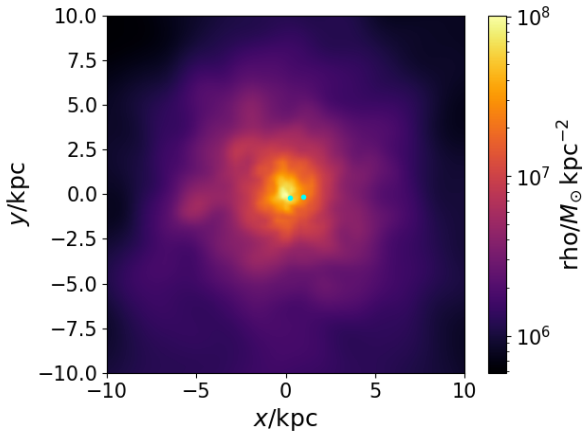

(f) Star configuration of the galaxy ID : 1064 with a width = 20 kpc; DM in purple and stars in green

Figure 4.3

The dark matter halos are shown below at a zoom-out large enough to appreciate the parent galaxy from which the satellite galaxies orbit. The parent galaxy with # ID: 116 has the largest dark matter halo, while the other two parent galaxies have dark matter halos of width ≈ 40 $[kpc]$.

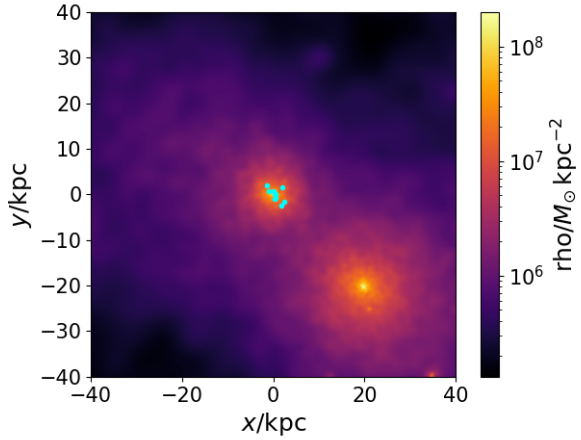

(a) Satellite dark galaxy with # ID: 746 and his parent galaxy with # ID: 178

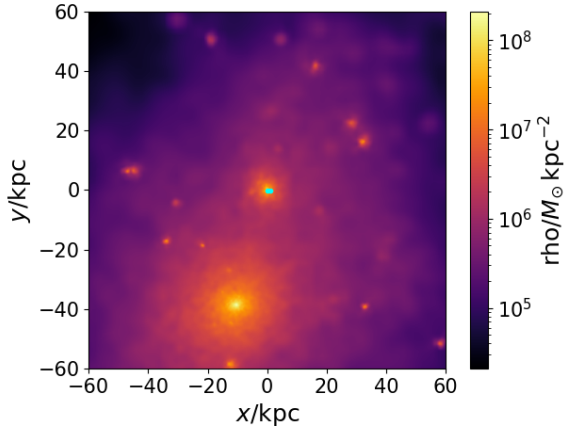

(b) Satellite dark galaxy with # ID: 1064 and his parent galaxy with # ID: 116

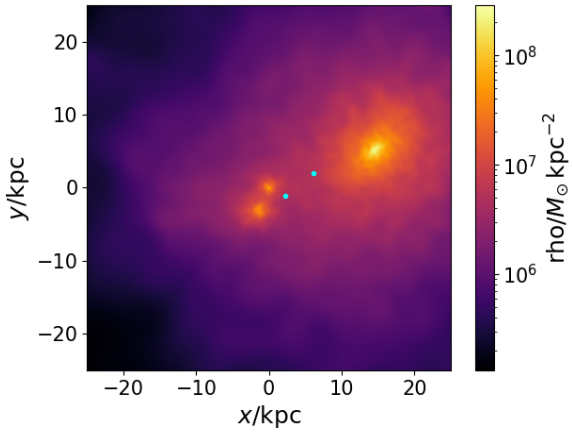

(c) Satellite dark galaxy with # ID: 5129 and his parent galaxy with # ID: 146

Figure 4.4

4.2. Properties of the Dark Galaxies

We have found the coordinates (x, y, z) of the dark galaxies given by the simulation **37_11**, and we have also obtained their virial radii. With these coordinates we have calculated the relative distances of the ten galaxies with respect to Milky Way and Andromeda, where the coordinates of these two galaxies have also been previously found. With this information it has been possible to make radial distributions of MW and M31 with respect to the dark galaxies.

ID	Xc [Mpc]	Yc [Mpc]	Zc [Mpc]	MW Distance [Mpc]	M31 Distance [Mpc]	Rvir [kpc]
273	70.66	74.02	67.56	3.86	3.32	36.09
278	70.05	71.44	70.16	3.69	2.88	35.85
370	63.71	74.12	71.78	4.72	5.26	31.78
393	68.59	69.12	67.26	6.4	5.75	30.84
398	70.91	74.0	67.13	4.36	3.82	31.03
691	70.75	73.95	67.17	4.23	3.7	25.37
746	68.84	74.36	72.03	1.68	1.78	14.12
804	68.4	75.67	67.11	3.54	3.6	23.85
1064	65.65	77.13	69.06	3.86	4.57	21.51
5129	65.8	77.16	69.38	3.68	4.42	8.4

Table 4.2: Coordinates and virial radius of the dark galaxies in simulation 37_11 and distances of these galaxies from the Milky Way and Andromeda.

The dark galaxies lie within approximately 6 $[Mpc]$ of MW and M31. Firstly, for the Milky Way case the set of dark galaxies with # ID : **273, 278, 370, 398, 691, 804, 1064** and **5129**, are at a distance of approximately 4 $[Mpc]$, however, the galaxy with # ID: **746**, is the closest to MW, with a minimum distance of 1. 68 $[Mpc]$, on the other hand, the galaxy with # ID: **393**, is the farthest from MW with a maximum distance of 6.4 $[Mpc]$. Secondly, in the case of Andromeda, the galaxies with # ID: **746** and **393**, as for MW, are the galaxies that are furthest and closest to M31, being at distances of 1. 78 $[Mpc]$ and 5.75 $[Mpc]$ respectively, on the other hand, the remaining group of galaxies are in a wider range of distances, between approximately 3 $[Mpc]$ and 5 $[Mpc]$.

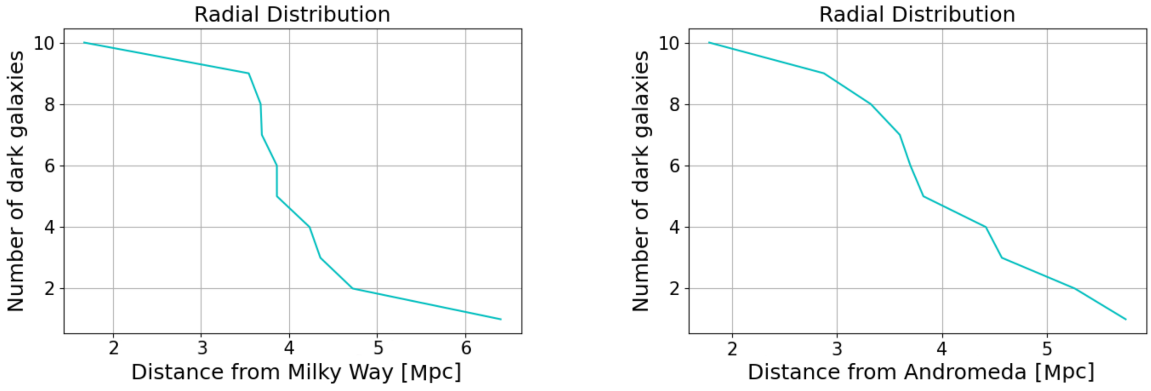

(a) Milky Way (b) Andromeda

Figure 4.5

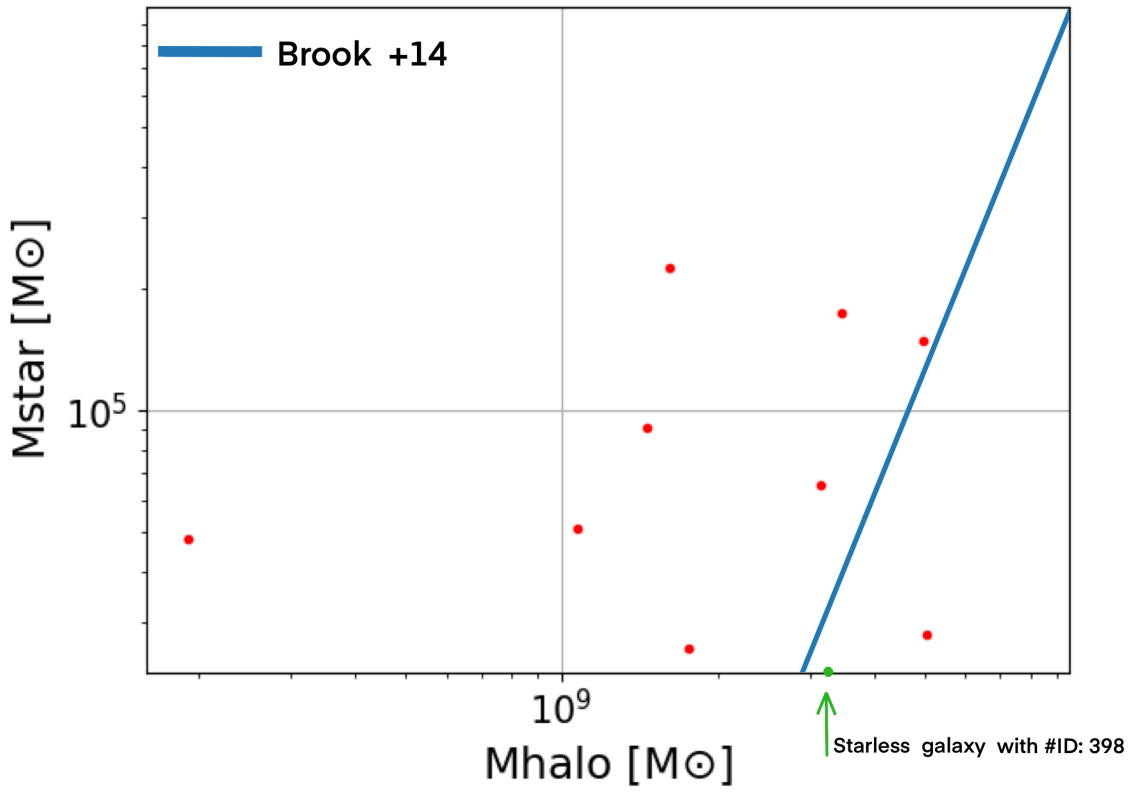

Figure 4.6: Stellar mass and halo mass relation of the dark galaxies with respect to Brook + 14. The only starless galaxy is shown in green and lies on the x-axis, which corresponds to an Mstar=0, the rest of the galaxies that have stellar mass are shown as red dots.

The relation of stellar mass to dark matter halo mass of dark galaxies has been obtained and compared with Brook +14, which represents the mean of the stellar mass to dark matter halo mass relations of galaxies in general. As can be seen, most of the dark galaxies do not present an unusual behaviour, those that are close to the average but above it, present less dark matter mass than they should considering the amount of star mass they possess, this is curious because what characterises these galaxies is precisely their low stellar presence, but it seems that this quality is not so special because it is what is expected considering the halo mass they possess. If we focus on the galaxy (red dot) below the mean line, in this case, the amount of stellar mass it has is lower than it should have, given the mass of its halo. Finally, there are the two most peculiar galaxies, especially one of them, these galaxies are the ones with the # ID: **5129** (red dot closest to the y-axis) and # ID: **398** (green dot on the x-axis, indicating that its stellar mass is zero). The peculiarity of **5129** is how little dark matter mass it has relative to its stellar mass, which are $0.19 \cdot 10^9$ M⊙ and $4.83 \cdot 10^4$ M⊙ respectively, again the opposite of what is expected for this type of galaxy, but in this case it is more pronounced. Then there is the **398** galaxy, the most special case, the stellar mass to halo mass relation of this galaxy is completely out of line with the average, as it does not have a single star particle.

4.3. Temperature and density of gas in dark galaxies

In order to find an explanation for the apparent lack of stars in dark galaxies, the temperature and density of gas in each of these galaxies has been studied. In order to carry out this analysis, galaxies must have more than one unit of gas particles, so those with the # ID: **273, 370, 393, 398, 746, 804, 5129** are the ones with which this study can be carried out.

One of the conditions for gas particles to form stars is that the temperature of the gas is 'cold'. In cosmological simulations such as HESTIA, this means that the temperature of the gas must be close to 10^4 [K]. Above that temperature, the gas is already considered to be hot. The reason that cold gas is able to generate stars is that the gas collapses on itself under gravity due to its low internal pressure. In hot gas, on the other hand, the gravitational force that generates the collapse is counteracted by the high internal pressure of the gas. The pressure of the hot gas is so high because of the high thermal energy it possesses.

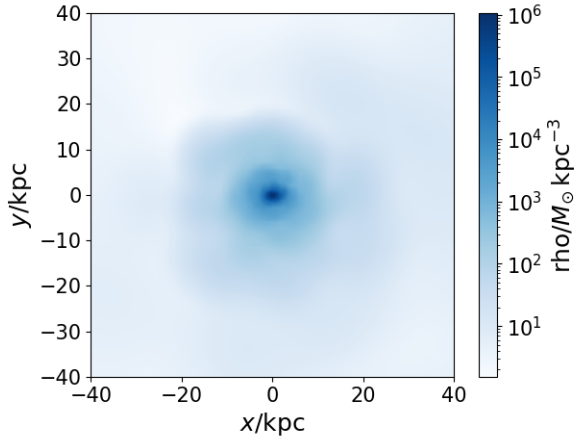

(a) Gas distribution of the galaxy with ID: 273

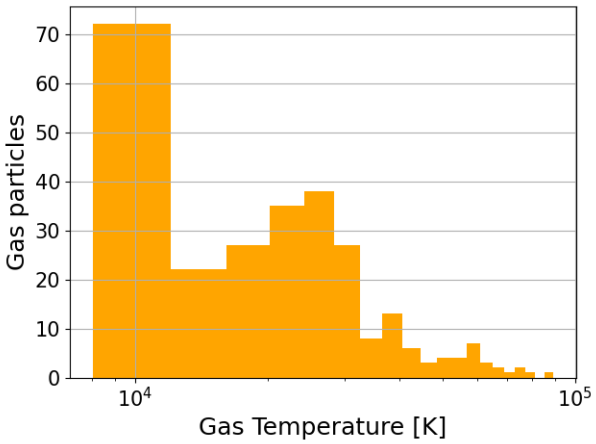

(b) Gas temperature histogram with 276 gas particles

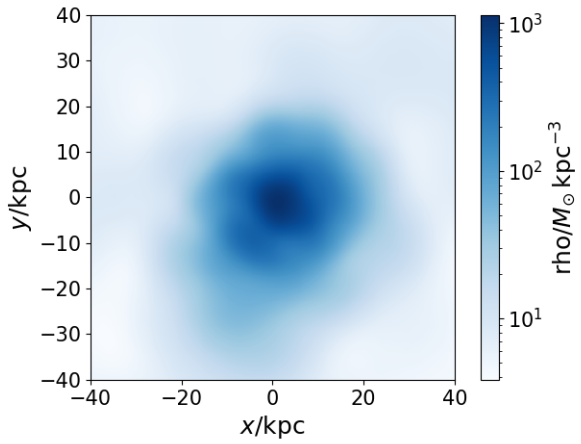

(c) Gas distribution of the galaxy with ID: 370

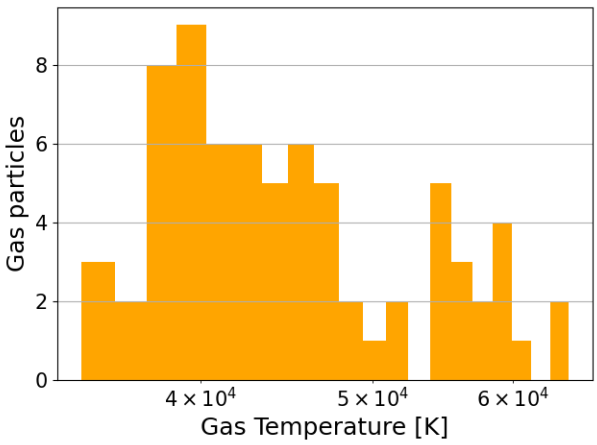

(d) Gas temperature histogram with 72 gas particles

Figure 4.7

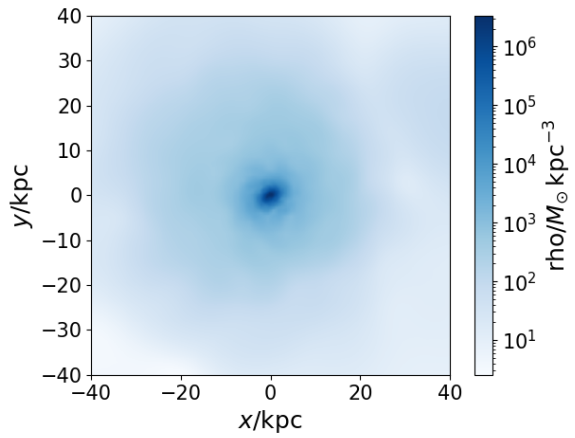

(a) Gas distribution of the galaxy with ID: 393

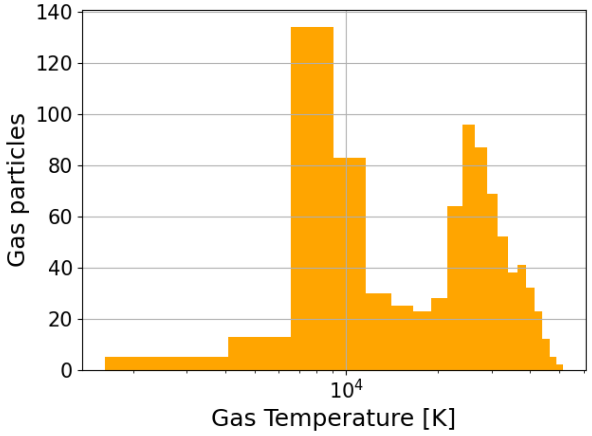

(b) Gas temperature histogram with 862 gas particles

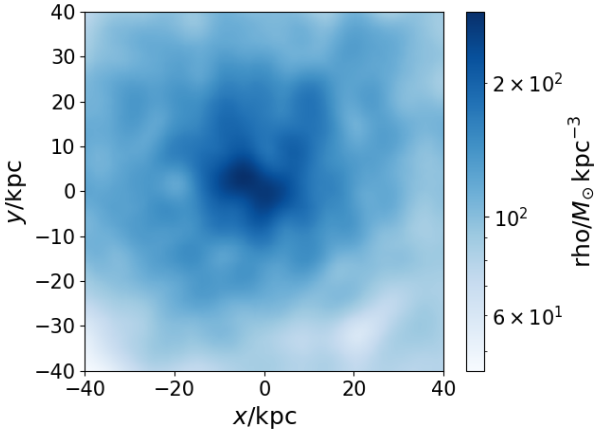

(c) Gas distribution of the galaxy with ID: 398

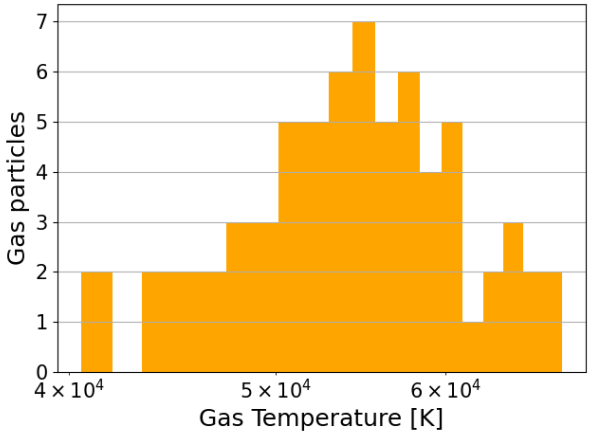

(d) Gas temperature histogram with 67 gas particles

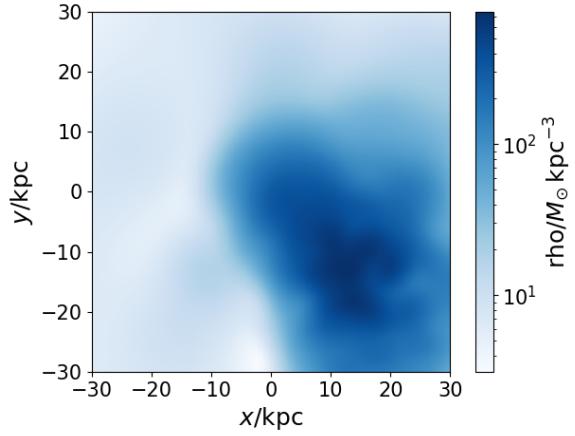

(e) Gas distribution of the galaxy with ID: 746

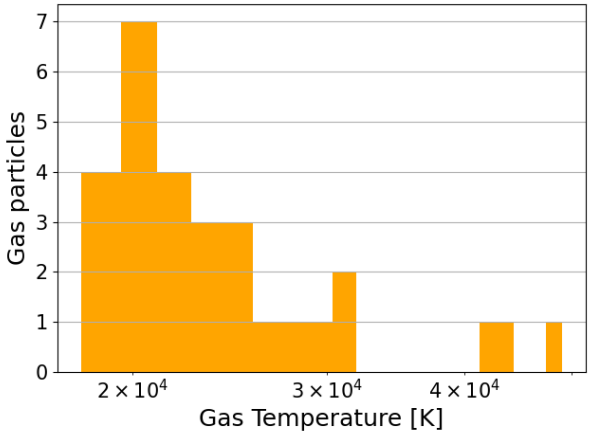

(f) Gas temperature histogram with 29 gas particles

Figure 4.8

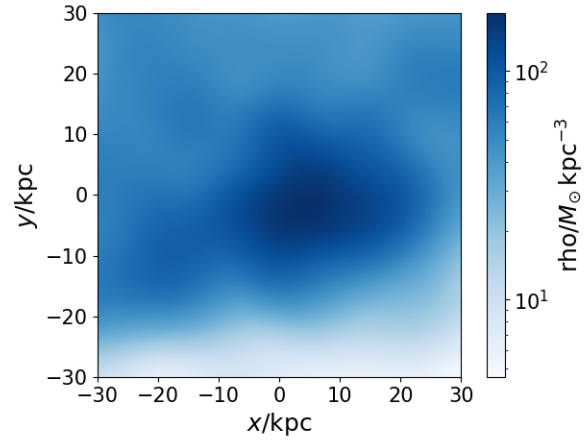

(a) Gas distribution of the galaxy with ID: 804

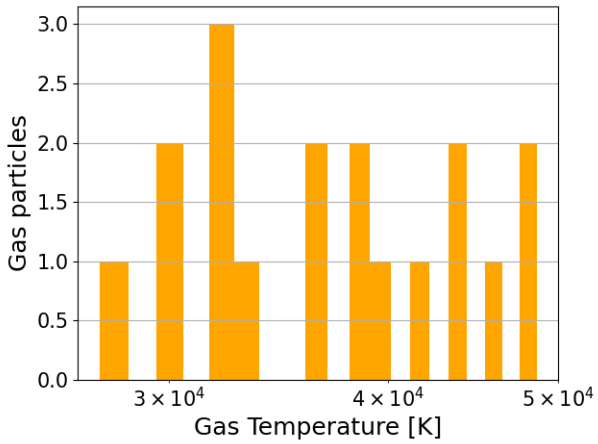

(b) Gas temperature histogram with 18 gas particles

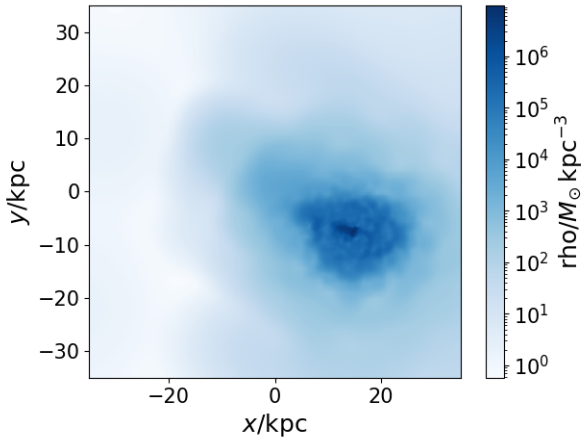

(c) Gas distribution of the galaxy with ID: 5129

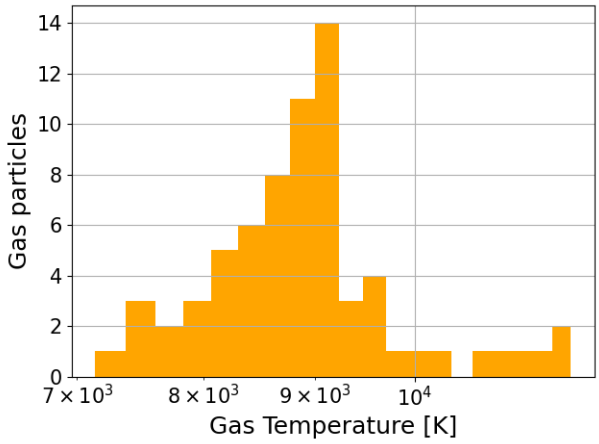

(d) Gas temperature histogram with 69 gas particles

Figure 4.9

The gas halos of the dark galaxies have been obtained together with a histogram representing the temperature of the gas particles in each of them. It can be seen that all the galaxies have cold gas, because the gas particles have temperatures of 10^4 [K]. Moreover, the dark galaxy with the highest gas temperature is the one with # ID: **273**, but even so, it does not qualify as hot gas. Therefore, the gas should generate stars.

With respect to the gas halos, the ones with the highest gas density are those with the highest number of gas particles, as in the case of galaxies with # ID: **273** and **393**, where the areas of the halo with the highest gas density reach values of approximately 10^6 $[\frac{M_\odot}{kpc^3}]$. On the other hand, galaxies with fewer gas particles, such as those with #ID: **370, 398, 746** and **804**, present lower gas densities, where the highest density values they possess are between 10^2 $[\frac{M_\odot}{kpc^3}]$ and 10^3 $[\frac{M_\odot}{kpc^3}]$. The exception is **5129**, which despite having a similar number of gas particles to galaxies **370** and **398**, the density of most of the gas particles in **5129** is

much higher than the densities of the other two galaxies.

It must be taken into account that for gas to form stars, it is not enough for it to be cold, it must also be dense, so the density is studied in more detail. In HESTIA the gas density at which stars start to form is $n_{thres} = 0.13$ $[\frac{amu}{cm^3}]$, but because the follow images are on a logarithmic scale, the limit value above at which the gas density forms stars is $\log_{10}(n_{thres})$ = -0.89 $[\frac{amu}{cm^3}]$.

For the galaxies **273** and **393** two-dimensional histograms have been obtained where the temperature and density of the gas particles are plotted. Each point represented is a set of gas particles with similar characteristics, if the point has a lighter colour, it means that there is a larger amount of gas particles being represented by that point. For the rest of the galaxies, a two-dimensional histogram could not be obtained because the number of gas particles they possess is not large enough.

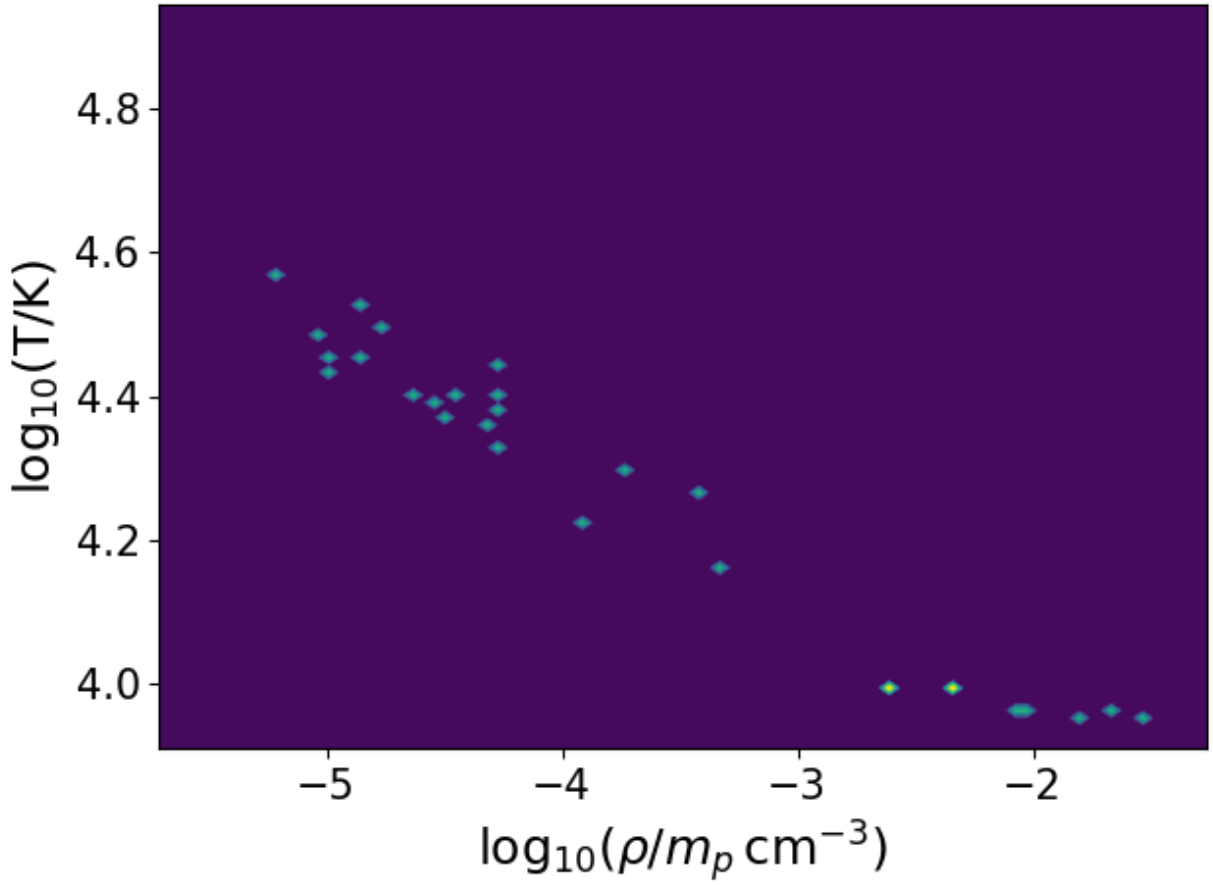

Figure 4.10: 2D histogram of temperature vs gas density of the galaxy with # ID: 273

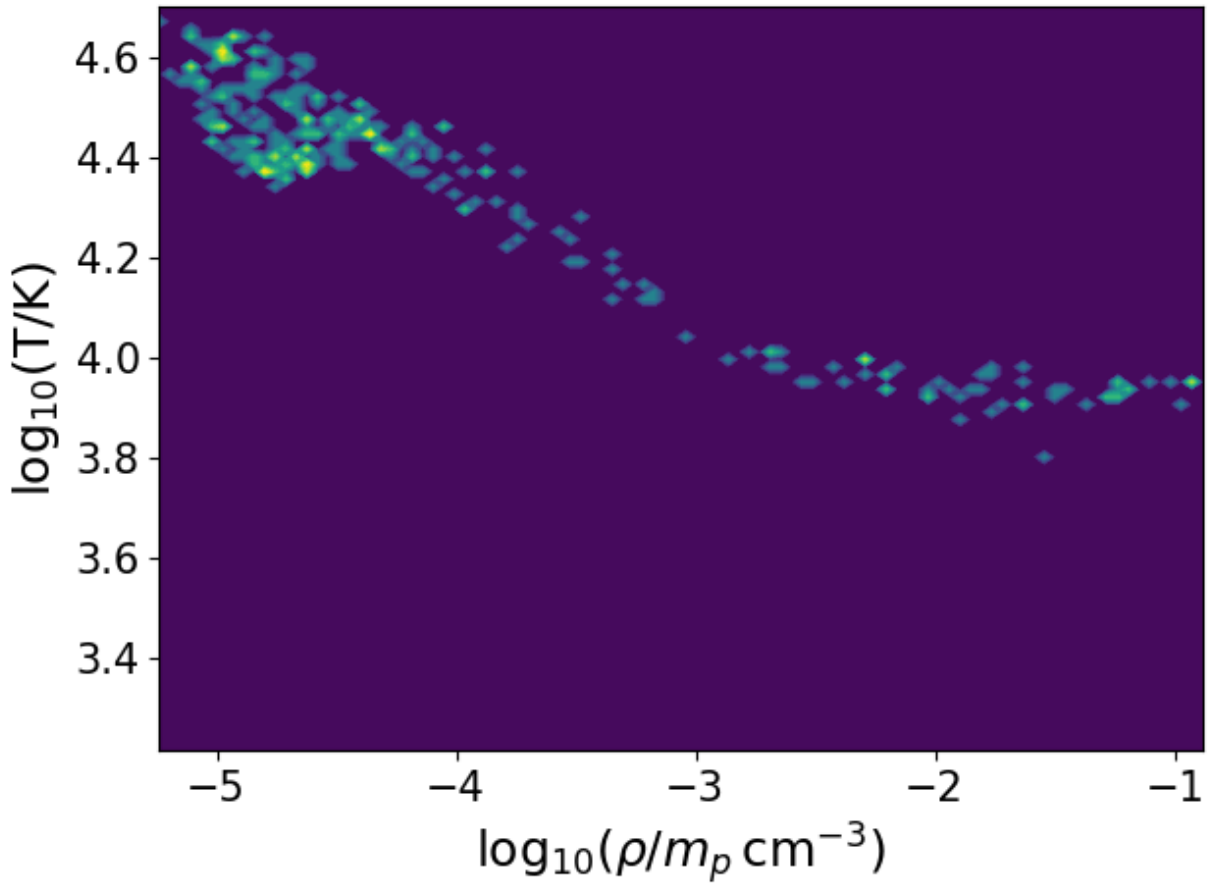

Figure 4.11: 2D histogram of temperature vs gas density of the galaxy with # ID: 393

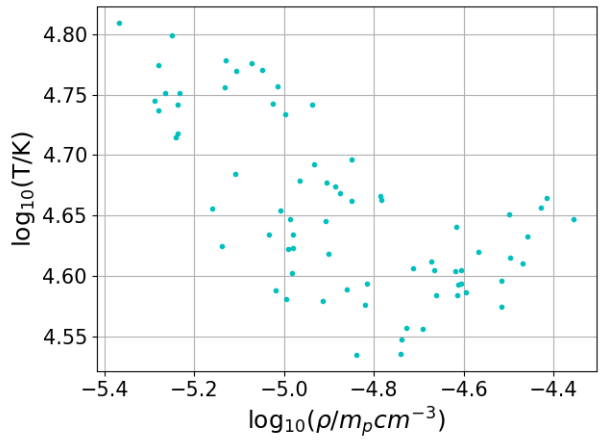

(a) Temperature vs gas density of the galaxy with # ID: 370

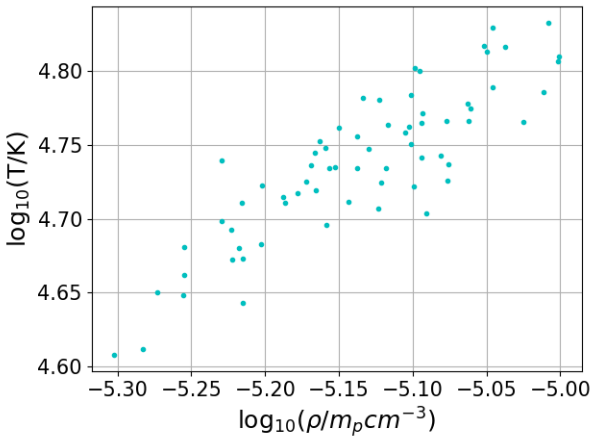

(b) Temperature vs gas density of the galaxy with # ID: 398

Figure 4.12

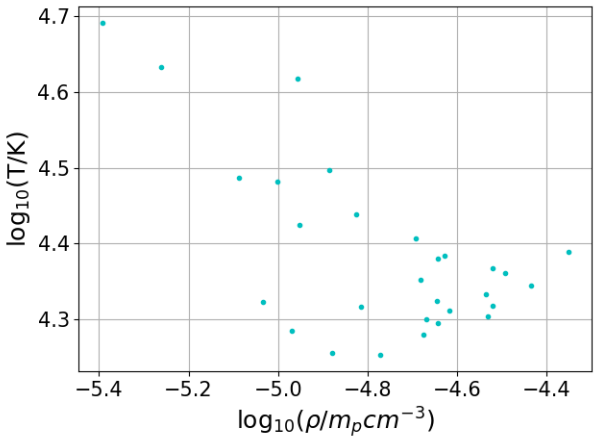

(a) Temperature vs gas density of the galaxy with # ID: 746

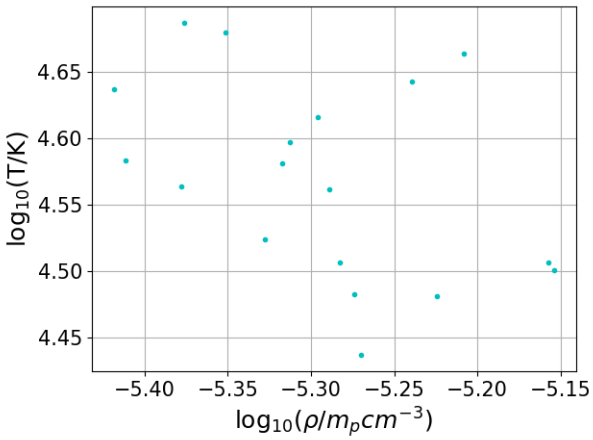

(b) Temperature vs gas density of the galaxy with # ID: 804

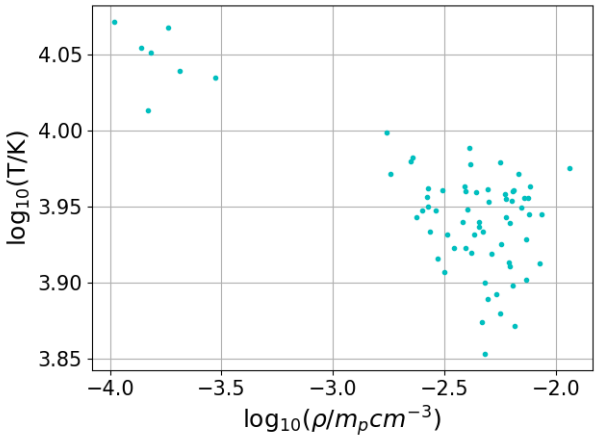

(c) Temperature vs gas density of the galaxy with # ID: 5129

Figure 4.13

In general terms, all dark galaxies have gas densities of several orders of magnitude lower than that necessary to generate stars. As can be seen, the hotter the gas, the less density it presents. This behaviour is different for the starless galaxy (the one with # ID: **398**), where the denser gas particles have a higher temperature, however, one explanation for this behaviour could be the small range in which temperature and density are represented. In the galaxy with # ID: **804**, there is no clear behaviour in terms of the densities and temperatures of its gas particles, possibly due to the scarcity of gas particles in this galaxy. As for the galaxies with the densest gas particles, we find those with # IDs: **273, 393** and **5129**. Of the three galaxies, the **5129** galaxy has the fewest gas particles, and those with the highest densities are between the -2.5 to -2 range. With respect to the **273** and **393** galaxies, they have the highest amount of gas particles of all dark galaxies and the range of their gas densities are between -5 and -2 for **273** and between -5 and -1 for **393**. Therefore, even for the case of the **393** galaxy, which has some of the densest gas particles of all, their densities do not go beyond the limit of -0.89, thus failing to generate stars.

5. Conclusions

En el TFG se han conseguido diez galaxias oscuras donde se han analizado aspectos específicos como sus masas estelares, sus masas de halo de materia oscura y las densidades y temperaturas de sus partículas de gas, con el objetivo de entender el por qué estas galaxias presentan tan poca masa estelar. Se ha concluido que uno de los factores determinantes es el gas, que a pesar de ser frío es poco denso, impidiendo la formación de estrellas

Through the high-resolution 37_11 HESTIA simulations, dark galaxies have been found for the first time, where most of them have stellar masses of 10^4 M$\odot$ and even one of them has no stars. This is in agreement with the recently published papers by Benitez-Llambay y Navarro, 2023 and Smith et al., 2024, where the former presents observational data of a system that does not have stars but does have dark matter and gas; and the second, exposes the existence of a satellite galaxy of MW with a stellar mass well below the ordinary, being 6 M$\odot$. Therefore, it is likely that as research in this sector progresses, more observational data can be obtained from galaxies with stellar masses similar to those presented in this TFG or even be able to find a galaxy with zero stellar mass for the first time.

A peculiarity that these dark galaxies have that makes them even more special is that their gas is cold and not dense, which is why they do not form stars.

With regard to future studies that can be carried out with the information from the dark galaxies obtained, an analysis of the history of each of the dark galaxies can be made, studying where they come from and why they have such peculiar properties. One possibility that explains the low amount of stellar mass they have could be due to the fact that they are back-splash galaxies, that is, galaxies that have passed through a cluster of galaxies, now being on the periphery and because of the interactions it had with the other galaxies, their gas has dispersed or their stars have been stripped. An example of a process that could caused this dispersion of the gas or stars is the tidal force.

Observational data on dark galaxies similar to those obtained in this TFG could be obtained in the local group. There are surveys that search for neutral hydrogen distributions in the nearby universe, such as the Arecibo Legacy Fast ALFA (ALFALFA) Survey (Giovanelli et al., 2005). This survey specifically uses the Arecibo radio telescope in Puerto Rico to identify HI concentrations. If there were a small amount of neutral hydrogen it would not be possible to detect it, but in our case, because the gas is cold, the approximate HI per galaxy is around 10^6 M$\odot$, so if it exists in the universe, it would be possible to find this type of galaxy through its neutral hydrogen. However, the concentration of HI found must have an associated dark matter halo in order to be considered a galaxy. With this in mind, I hope that in the not too distant future, observational data can be obtained from these types of galaxies in our cosmos, so that we can increase our understanding and even discover more interesting properties of them.

Acknowledgement

I would like to thank Arianna Di Cintio for clarifying my doubts, encouraging me and guiding me throughout the whole TFG. I'd also like to thank Elena Arjona Gálvez for her help at the beginning of the TFG, where she helped me understand in general the operation of the HESTIA simulation and with the installation process of pynbody.

References

Huang, Y. et al. (2016). "The Milky Way's rotation curve out to 100 kpc and its constraint on the Galactic mass distribution". En: *Monthly Notices of the Royal Astronomical Society* 463.3, págs. 2623-2639.

Chemin, L., C. Carignan y T. Foster (2009). "H i Kinematics and dynamics of messier 31". En: *The Astrophysical Journal* 705.2, pág. 1395.

McConnachie, A. W. (2012). "The observed properties of dwarf galaxies in and around the Local Group". En: *The Astronomical Journal* 144.1, pág. 4.

White, S. D. y M. J. Rees (1978). "Core condensation in heavy halos: a two-stage theory for galaxy formation and clustering". En: *Monthly Notices of the Royal Astronomical Society* 183.3, págs. 341-358.

Klypin, A., A. V. Kravtsov, O. Valenzuela y F. Prada (1999). "Where are the missing galactic satellites?" En: *The Astrophysical Journal* 522.1, pág. 82.

Moore, B. et al. (1999). "Dark matter substructure within galactic halos". En: *The Astrophysical Journal* 524.1, pág. L19.

De Blok, W. y A. Bosma (2002). "High-resolution rotation curves of low surface brightness galaxies". En: *Astronomy & Astrophysics* 385.3, págs. 816-846.

Libeskind, N. I. et al. (ago. de 2020). "The ¡scp¿hestia¡/scp¿project: simulations of the Local Group". En: *Monthly Notices of the Royal Astronomical Society* 498.2, págs. 2968-2983. ISSN: 1365-2966. DOI: 10.1093/mnras/staa2541. URL: http://dx.doi.org/10.1093/mnras/staa2541.

Benitez-Llambay, A. y J. F. Navarro (sep. de 2023). "Is a Recently Discovered H i Cloud near M94 a Starless Dark Matter Halo?" En: *The Astrophysical Journal* 956.1, pág. 1. DOI: 10.3847/1538-4357/acf767. URL: https://dx.doi.org/10.3847/1538-4357/acf767.

Navarro, J. F. (1996). "The Structure of cold dark matter halos". En: *Symposium-international astronomical union*. Vol. 171. Cambridge University Press, págs. 255-258.

Smith, S. E. T. et al. (ene. de 2024). "The Discovery of the Faintest Known Milky Way Satellite Using UNIONS". En: *The Astrophysical Journal* 961.1, pág. 92. DOI: 10.3847/1538-4357/ad0d9f. URL: https://dx.doi.org/10.3847/1538-4357/ad0d9f.

Springel, V. (2010). "E pur si muove: Galilean-invariant cosmological hydrodynamical simulations on a moving mesh". En: *Monthly Notices of the Royal Astronomical Society* 401.2, págs. 791-851.

Pakmor, R. et al. (2016). "Improving the convergence properties of the moving-mesh code AREPO". En: *Monthly Notices of the Royal Astronomical Society* 455.1, págs. 1134-1143.

Grand, R. J. et al. (2017). "The Auriga Project: the properties and formation mechanisms of disc galaxies across cosmic time". En: *Monthly Notices of the Royal Astronomical Society* 467.1, págs. 179-207.

Collaboration, P. et al. (2014). "Planck 2013 results. XVI. Cosmological parameters". En: *A&A* 571, A16.

Hubble, E. P. (1979). "Extra-galactic nebulae". En: *A Source Book in Astronomy and Astrophysics, 1900–1975*. Harvard University Press, págs. 716-724.

Rubin, V. C., W. K. Ford Jr y N. Thonnard (1978). "Extended rotation curves of high-luminosity spiral galaxies. IV-Systematic dynamical properties, SA through SC". En: *Astrophysical Journal, Part 2-Letters to the Editor, vol. 225, Nov. 1, 1978, p. L107-L111.* 225, págs. L107-L111.

Giovanelli, R. et al. (dic. de 2005). "The Arecibo Legacy Fast ALFA Survey. I. Science Goals, Survey Design, and Strategy". En: *The Astronomical Journal* 130.6, págs. 2598-2612. ISSN: 1538-3881. DOI: 10.1086/497431. URL: http://dx.doi.org/10.1086/497431.